

Trapping Highly Reactive Photo-Induced Charge-Transfer Complex Between Amine and Imide by Light

Wenhuan Huang,^{1,2} Xiaolong Zhang,¹ Hao Su,¹ Baicheng Zhang,^{1,2} Airong Feng,³ Jun Jiang,^{1,2} Biao Chen,^{1*} and Guoqing Zhang^{1,2,*}

¹Hefei National Research Center for Physical Sciences at the Microscale, University of Science and Technology of China, 96 Jinzhai Rd., Hefei, 230026, China

²Hefei National Laboratory, University of Science and Technology of China, University of Science and Technology of China, Hefei 230088, China

³Instruments Center for Physical Science, University of Science and Technology of China, 96 Jinzhai Rd., Hefei, 230026, China

*Correspondence: biao.chen@ustc.edu.cn

*Correspondence: gqzhang@ustc.edu.cn

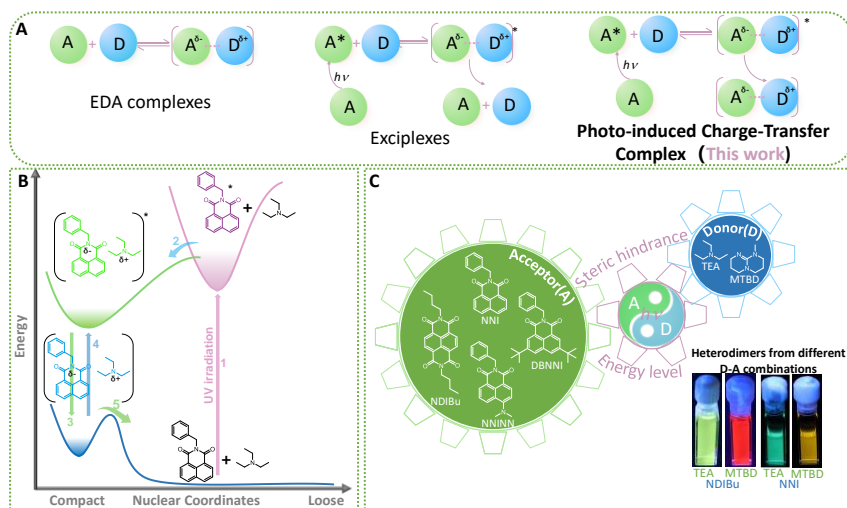
SUMMARY

Complexation between two organic molecules can occur either for strong electron donor-acceptor pairs in the ground state known as charge-transfer complexes (CTCs), or for pairs of lesser strength in the excited state such as excimers and exciplexes. However, the characterization of chemically distinct CTCs in solution remains elusive. Here, we report a light-induced, solution-persistent 1:1 CTC between an amine and an imide. The pair is not associated in the ground state at room temperature prior to light exposure. The presence and exact molecular compositions of the CTCs could be directly obtained from high-resolution mass spectrometry. Additional spectroscopic and computational evidence reveals that a kinetically trapped ground-state pair is formed following an exciplex-like process between the amine and the imide after photo-excitation. We show that such a photo-induced complex can be used to conduct photochemistry and store photon energy for producing otherwise photochromic products in the dark.

keywords: Charge-Transfer Complex, photo-induced, photopolymerization, photoconversion, carbon dioxide reduction

INTRODUCTION

Charge transfer (CT), during which an electron partially or completely relocates to a different region, is perhaps the most important physical process for chemistry, given that it dictates how molecules and materials interact, both physically and chemically.¹ Two molecules that are strongly coupled by CT are usually referred to as an electron donor-acceptor complex;² the coupling may occur in the ground state, in which an electron donor-acceptor (EDA)-, or CT-complex^{3,4} (CTC, Scheme 1a) forms to give rise to a new ground state. The coupling can also proceed in the excited state only, where a transiently excited complex^{5,6} (exciplex, Scheme 1a) quickly decays into two weakly interacting or even repelling ground-state molecules without new ground states manifested spectroscopically. With the ability to significantly red-shift the ultraviolet absorption of individual donor or acceptor molecules, CTCs have been used for visible light-initiated synthesis,^{7,8} such as C-H activation,⁹ cycloaddition,^{10,11} substitution,^{12,13} and rearrangement.¹⁴ On the other hand, as a superposition of singlet and triplet excited states, exciplexes can be beneficial for spin-related charge injection and migration, such as organic light-emitting diodes,^{15,16} semiconductors,¹⁷ and photovoltaic devices.^{18,19} Unfortunately, CTCs are



Scheme 1. The formation and regulation of PCTC

(A) Formation of EDA complexes, exciplexes and photo-induced charge-transfer complex. (B) Schematic diagram of PCTC indicating a kinetically trapped state (1-UV irradiation, 2-Formation of an exciplex-like state, 3-Formation of a ground-state CTC, 4-Re-excitation of PCTC, 5-Dissociation of PCTC into its constituent molecules). (C) Various chemical structures of acceptor and donor components of PCTCs resulting in different photoluminescence colors in solution under argon.

chemically elusive in solution, which poses a significant challenge for elucidating their properties holistically and thus prevents further harnessing their application potentials.

Ground-state CTCs²⁰ usually form immediately upon contact between electron donor and acceptor molecules, indicating very low kinetic energy barriers and thus presumably very rapid dissociation rate. According to the Marcus electron transfer theory,²¹ however, if the donor HOMO energy is decreased, or if the acceptor energy is decreased, or both, the kinetic energy barrier starts to become elevated and thus prevents the formation of CTCs in the ground state. In such a scenario, photons may be supplied as an external energy source to help surmount the kinetic energy barrier of the CTCs, similar to adiabatic photochemical reactions. Assuming that the process could occur in organic solutions, a stable CTC may be obtained via $D^* + A \rightarrow CTC$ or $D + A^* \rightarrow CTC$, as long as the kinetic barrier is significantly higher than k_bT for the dissociation reaction $CTC \rightarrow D + A$, where $D(A)$ and $D^*(A^*)$ represent the ground-state and excited state donor(acceptor) molecules, respectively (Scheme 1a). Nevertheless, to the best of our knowledge, there have been no reports on stable ground-state complex formation necessitated by light, *i.e.*, a CTC as a product of a relaxed exciplex. In this study, we present the direct observation of photo-induced charge-transfer complex (PCTC, Scheme 1) formation between an amine and an imide, which are initially unpaired in the ground state, in organic solution at room temperature.

The imide, N-substituted 1,8-naphthalimide (NNI), is a strong electron accepting molecule exhibiting a plethora of interesting physical, chemical and biological activities,^{22,23} such as strong room-temperature phosphorescence,^{24,25} photocatalysis,^{26,27} and anti-fungal properties,²⁸ and has been extensively studied over the past few decades. Recently, we showed that excited-state CT between methoxyphenyl and NNI significantly can boost the phosphorescence yield of NNI.²⁹ When the donor group is further strengthened, in the case of an enolate, deeply colored supramolecular CTC gels could thus be obtained from the otherwise colorless NNI and enolate polymeric components, respectively.³⁰ In the current study, we first present the observation of light-induced CTC between NNI and triethylamine (TEA), and then extend the condition to amines and imides of different chemical structures (Scheme 1c). In general, the amine/imide mixtures do not show typical signatures of CTC in the ground state in solution (*e.g.*, no new absorption or static fluorescence quenching) but become strongly associated as a solution-stable, spectroscopically distinct pair after UV irradiation under inert atmospheres such as argon. A combination of spectroscopic techniques including high-resolution mass spectrometry (HRMS), nuclear magnetic resonance (NMR), electron paramagnetic resonance (EPR), and time-resolved 3D photoluminescence methods are used to characterize the CTCs in solutions. Theoretical calculations are also performed to

shed light on plausible molecular arrangements between NNI and amine in a charge-transfer complex. Based on both experimental and theoretical results, a physical model for this photo-induced charge-transfer complex (PCTC) is proposed, which is defined as a persistent ground-state molecular complex pair necessitated by light and the presence of which must be experimentally verifiable by HRMS.

RESULTS AND DISCUSSION

Generation and spectroscopic characterization of PCTC

We first noted that, shown in Figure 1a, when the CH₃CN solution of triethylamine (TEA) and an NNI derivative (NNI) is irradiated with a 365-nm LED lamp under an argon atmosphere, it gradually shows strong green photoluminescence to the naked eye. Such changes indicate the presence of new chemical species, which were first examined with UV-Vis absorption ($\lambda_{\text{abs}} = 400$ nm) and photoluminescence ($\lambda_{\text{PL}} = 500$ nm) spectra. The maximal absorption or emission values are substantially red-shifted compared to the NNI/TEA mixture prior to photo-radiation ($\lambda_{\text{abs}} = 333$ nm; $\lambda_{\text{PL}} = 377$ nm). Oxidations or aggregation of amines have been known to produce obscure luminescent products;³¹ luminescent reduction products of Meisenheimer complexes formed by NNI derivatives have been recently observed by Nocera et al.³² To identify the strongly luminescent species, absorption spectra at two different NNI concentrations (0.1 mM and 1 mM) were performed (Figure 1b), clearly showing that the majority of the NNI molecules were chemically converted, which should rule out the former hypothesis. The emergence of the new species is better visualized via 3D excitation-emission correlated fluorescence spectra, which reveal a dramatic difference in the region of maximal intensity before and after UV treatment (Figure 1c). Specifically, the 3D peak (red region) characteristics of NNI fluorescence, is essentially identical between NNI or NNI/TEA prior to UV treatment. After UV exposure, however, the initial peak largely diminished for the NNI/TEA solution and is replaced by an entirely new peak with much lower-energy coordinates in the 3D graph (Figure S1). Incidentally, it was noted that the absorption and emission spectra of the newly generated species, which can be re-excited with visible light beyond 400 nm under inert atmospheres (figure S2), are very similar to those of the 4-N,N-dimethyl-substituted NNI (NNINN, Figure S3). This similarity prompted us to consider whether a photochemical reaction could have occurred between the amine and the imide and could have given rise to the observed spectroscopic changes. However, the idea of a stable covalent chemical product, such as a classical Meisenheimer complex, was less compatible: when the UV treated solution of NNI/TEA was exposed to oxygen, the photoluminescence quickly dimmed within 3 min while that of the NNINN solution remained unchanged (Figure S4). Eventually, molecular oxygen could cause the new absorption and emission bands to retrogress to their pre-UV exposure states (Figure S5). This is in contrast to the reverse reaction of a typical Meisenheimer complex, which usually requires strong acid.

We then considered the possibility of a non-classical, Meisenheimer-complex-like structure and further probed the identity of the UV-generated chemical species. Surprisingly, despite the dramatic changes in UV spectrum, the ¹H-NMR revealed that the NNI/TEA mixture was essentially unchanged using *mesitylene* as an internal standard before and after UV exposure (Figure S6), again confirming the absence of typical covalent products. In a recent investigation³³ on how solvents influence the photophysical properties of an acridinium derivative, we noted the same spectroscopic features: the ¹H-NMR spectrum of the acridinium could maintain unaltered while its UV-absorption and photoluminescence (both fluorescence and phosphorescence) exhibit huge differences measured in different solvents. The observations were attributed to the formation of either weak or strong 1:1 ground-state coordination complexes between the acridinium cation and solvent molecules with lone-pair electrons, quantified by the titration method using a calorimeter. Consequently, we suspect that UV radiation of NNI in the presence of TEA might have resulted in a similar coordination complex, *i.e.*, photo-induced charge-transfer complex.

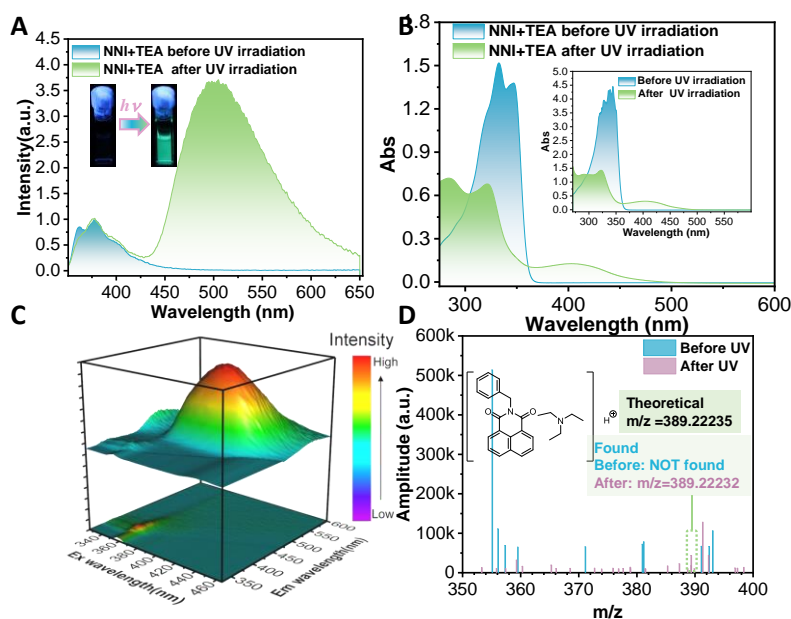


Figure 1. Spectroscopic characteristics of NNI/TEA mixture before and after UV treatment

(A) Steady-state photoluminescence spectra ($\lambda_{\text{ex}} = 335 \text{ nm}$) of the NNI/TEA mixture (NNI: $1 \times 10^{-4} \text{ M}$, TEA:10 eq. in CH_3CN) before and after UV irradiation under Ar.

(B) Absorption spectra of the NNI/TEA mixture before and after UV irradiation under Ar (NNI: $1 \times 10^{-4} \text{ M}$, TEA:10 eq., inset: NNI: $1 \times 10^{-3} \text{ M}$, TEA:10 eq. in CH_3CN).

(C) 3D excitation-emission correlated photoluminescence spectra of the NNI/TEA mixture before (bottom) and after (top) UV irradiation under Ar (NNI: $1 \times 10^{-4} \text{ M}$, TEA:10 eq. in CH_3CN).

(D) HRMS graphs with designated m/z ranges for CH_3CN solutions of the NNI/TEA mixture before and after UV irradiation to show that the relative amplitude of the CTC is not trivial. The solution sample was exposed to air immediately prior to and during the course of the HRMS measurement (NNI: $1 \times 10^{-4} \text{ M}$, TEA:10 eq.)

To provide direct experimental evidence for the presence of such a proposed PCTC species, we resorted to high-resolution mass spectrometry (HRMS). Given that PCTC is unstable in air, the UV-treated solution was injected into the spectrometry as quickly as possible. Fortuitously, the exact molecular weight of the NNI-TEA- H^+ formula (389.22232 Da) could be found with a relatively high amplitude. However, the value cannot be matched for the NNI/TEA mixture solution without UV irradiation (Figure 1d). Although HRMS could not be used to elucidate the molecular arrangement of the PCTC, we can nonetheless infer that the complex has substantial intra-complex CT character compared to the NNI fluorophore alone. Correspondingly, the luminescence lifetimes also manifest dramatic changes from short-lived radiative decay of the initial NNI/TEA mixture ($\tau = 2.41 \text{ ns}$ with non-exponential decay kinetics due to dynamic quenching by TEA) to much longer-lived, single-exponential decay kinetics of the NNI-TEA PCTC ($\tau = 17.3 \text{ ns}$, Figure S7).

To evaluate the impact of solvents on the inception and robustness of PCTC, we undertake an *in-situ* exploration and characterization of PCTC in various solvents (Figure S8-S10): Toluene (MB), Tetrahydrofuran (THF), Acetonitrile (MeCN), and Dimethyl Sulfoxide (DMSO). Specifically, in toluene the emission spectra and luminescent lifetimes remained largely unchanged pre- and post-UV irradiation, reflecting the absence of PCTC formation. This is corroborated by the lack of new absorption peaks in toluene before and after UV exposure. This result is interpreted as weak dimer/excplex formation between NNI and MB or with itself, reflected in the emission spectra of NNI in MB (broadened and structureless) prior to irradiation. Since the exciplex state is key to PCTC formation, disruption of this process is expected to prevent PCTC from forming. In contrast, other solvents like THF, MeCN, and DMSO all facilitated the formation of PCTC, as evidenced by the appearance of new emission and absorption peaks upon UV treatment. Notably, the luminescent lifetime increased and the emission wavelength of PCTC shifted to the red

region corresponding to the increasing polarity of the solvent, indicating the CT nature of PCTC (Figure S11). We also examined the NMR and EPR spectral behaviors of NNI in the presence of TEA within DMSO (Figures S12-S13). Our findings demonstrate that even in DMSO (a solvent with higher polarity than MeCN), the NMR spectra remained consistent before and after UV irradiation. Additionally, no EPR signal indicative of PCTC dissociation was detected. This suggests that while PCTC formation occurs in more polar solvents, these conditions do not necessarily lead to its dissociation.

Furthermore, we provide additional evidence affirming the existence of CTC, extending beyond HRMS. Initially, we synthesized a crosslinked polymer-bound TEA (CPEDA) and proceeded to immerse this insoluble polymer in a 0.1 mM solution of N-substituted naphthalimide (NNI) in acetonitrile. We then irradiated this system with UV light while also maintaining a control sample in the dark to compare the outcomes (Figure S14). After a 5-minute exposure, we removed the CPEDA from both solutions and measured the remaining NNI concentration via UV-Vis absorption spectroscopy. The results were quite revealing. In the absence of UV light, the absorption peak of NNI remained virtually unchanged upon extraction of CPEDA, suggesting no significant interaction or complex formation with NNI under dark conditions (Figure S15). Conversely, the solution that had been exposed to UV light showed a decrease by 8.9% in the absorption peak intensity of NNI after CPEDA was removed. This suggests that upon UV irradiation, CPEDA participates in the formation of PCTC with NNI (limited by surface area and diffusion kinetics in the crosslinked matrix). This is evidenced by the reduced NNI concentration in solution, indicating that a portion of the NNI molecules had been sequestered by the polymer support to form the PCTC (Figure S14).

Also, we conducted a series of experiments to monitor changes in the spectroscopic properties of PCTC upon the addition of extra NNI derivative equivalents. In the experiment, we systematically increased the concentration of NNI in a solution that had previously undergone UV irradiation to form PCTC (figureS16). We closely monitored the changes in UV absorption with each incremental addition of NNI. Our findings indicate that as the concentration of NNI increased, the intensity of its characteristic absorption peak correspondingly rose, suggesting an accumulation of NNI in the solution. However, the absorption peak intensity associated with PCTC remained largely unchanged, indicating that the presence of additional NNI did not significantly affect the PCTC absorption characteristics. These observations are consistent with a system where additional NNI does not partake in further reducing reactions.

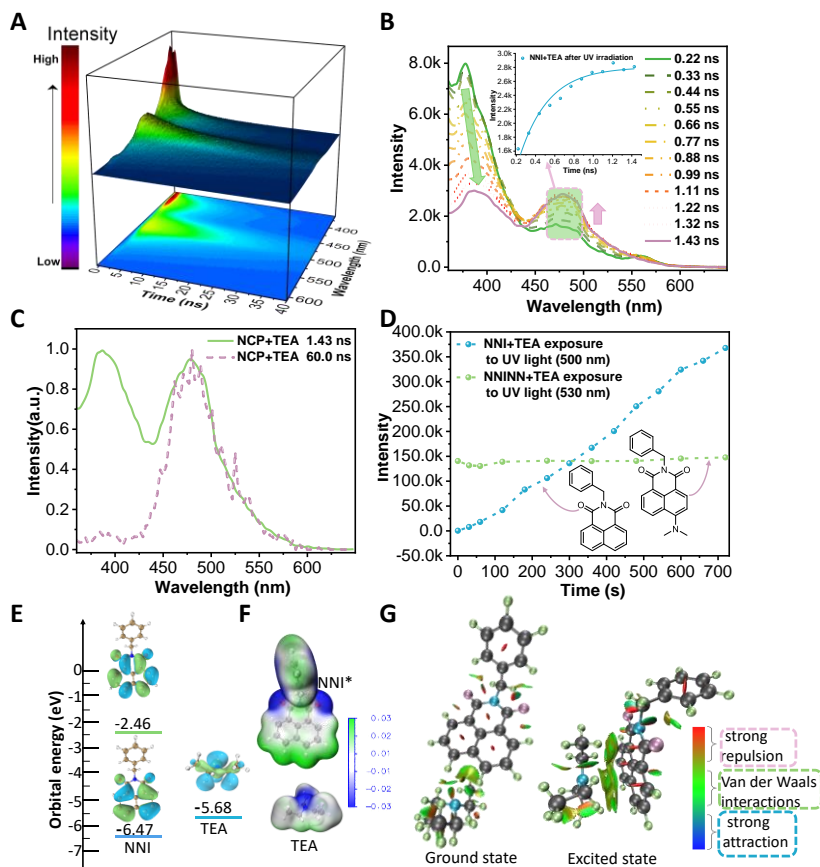


Figure 2. Evidence for the formation of PCTC

(A) The 3D surface (top) and contour plots (bottom) of time-resolved emission spectra (TRES) of the post-UV treatment NNI/TEA mixture (NNI: 1×10^{-4} M, TEA: 10 eq., Ex: 285 nm in CH_3CN).

(B) Emission spectral line series of NNI-TEA sliced from different delayed times after UV treatment under Ar in CH_3CN , inset: fitting with pseudo-first-order kinetics.

(C) Time-resolved emission spectra (1.43 ns, 60.0 ns) of NNI-TEA (NNI: 1×10^{-4} M, TEA: 10 eq., Ex: 285 nm).

(D) Relationship of emission spectra intensity vs. UV irradiation time (recorded at $\lambda = 500$ nm for NNI-TEA, $\lambda = 530$ nm for NNINN, NNI: 1×10^{-4} M, NNINN: 1×10^{-4} M, TEA: 10 eq. in CH_3CN).

(E) Energy levels of NNI and TEA, calculated at the B3LYP-D3BJ/6-31G (D, P) level in CH_3CN .

(F) Molecular electrostatic potential surface of NNI in excited state (NNI*), TEA in ground state computed at the B3LYP-D3BJ/6-31G (D, P) level.

(G) RDG mapped with isosurfaces (isovalue: 0.6); blue indicates strong attractive interactions and red indicates strong repulsive interactions.

The process of PCTC formation

How does the PCTC form? Since UV light is required to produce them, it is then plausible to assume that the complexes go through an exciplex-like state after NNI absorbs a UV photon and encounters a TEA molecule by diffusion. Therefore, time resolved emission spectroscopy (TRES) measurements can be used to provide more details on the bimolecular dynamics in the excited state. The populated band at ~ 500 nm, observed in the 3D surface and time-resolved intensity contours of the NNI/TEA mixture in CH_3CN (0.1 mM), is related to the fluorescence emitting state of the encounter exciplex [NNI-TEA]* (Figure 2a). The kinetics information can be extracted into Figure 2b, where sliced emission spectral lines are obtained from the intensity-wavelength plane in the time ranges of 0.22 ns–1.43 ns. Two peak maxima at ~ 380 nm and ~ 500 nm can be resolved from the onset of emission spectra to the end of the time period. As a function of time, the

intensity at ~500 nm increases and can be fitted with a pseudo-first-order or second-order kinetics (Figure S17), consistent with a bimolecular process. Concomitantly, the fluorescence of NNI at ~380 nm decreases and leads to an isoemissive point ~440 nm, suggesting the generation of PCTC at the cost of NNI over time. The two peaks at ~380 nm and ~500 nm can be isolated after 60 ns (Figure 2c), indicating that they do not originate from the same chemical component.

Theoretical evidence for the generation of PCTC

To understand why NNI and TEA could form a PCTC, theoretical calculations of energy levels for TEA, NNI, and NNINN were performed. The NNINN derivative was used as a control which cannot form PCTC with TEA under the same experimental condition (Figure 2d and Figure S18). The observation suggests that unsubstituted 4/5 positions are a foremost prerequisite for PCTC formation since the HOMOs of both NNI and NNINN are below that of the TEA (Figure 2e and Figure S18). To shed light on the site of coordination, Figure 2f shows the calculated electrostatic potential surfaces (ESP)³⁴ of excited state NNI* and ground-state TEA. The blue surfaces are characterized by higher electronic potential energy relative to the green ones. It can be seen that the electron-deficient region of NNI* is mainly distributed at the 3/4/5/6 positions of the naphthalene ring. On the other hand, the electron-rich region of TEA is mainly located on the N atom due to the lone-pair electrons. Consequently, the more electro-positive region of the NNI* can be attracted to the electro-negative area in TEA via intermolecular interactions near these sites.

To quantify the noncovalent interactions, calculations were performed in the Multiwfn program.³⁵ As shown in Figure 2g, the reduced electron density gradient (RDG)³⁶ can be used to provide evidence for the existence of intermolecular interactions such as attraction, repulsion, and van der Waals interactions. The calculation indicates that the binding energy of NNI and TEA in the excited state (-50.4 kcal/mol) is much larger than that of the pair in the ground state (-7.16 kcal/mol). It is also noted from the calculations that the PCTC formation could initiate by a strong interaction between the lone pair electrons and the π orbitals of the excited NNI*. Upon the transition of the PCTC from its excited state ([NNI-TEA] *) to the ground state by emitting a photon, the amine molecule rotates 90° from out of the aromatic plane and slides in between the 4 and 5 positions of the NNI ring in plane. The Gibbs free energy change ($\Delta G = G_{es} - G_{gs}$) during the transition is determined to be 36.4 kcal/mol, or 785 nm in photon energy, a reasonable value within the error range.

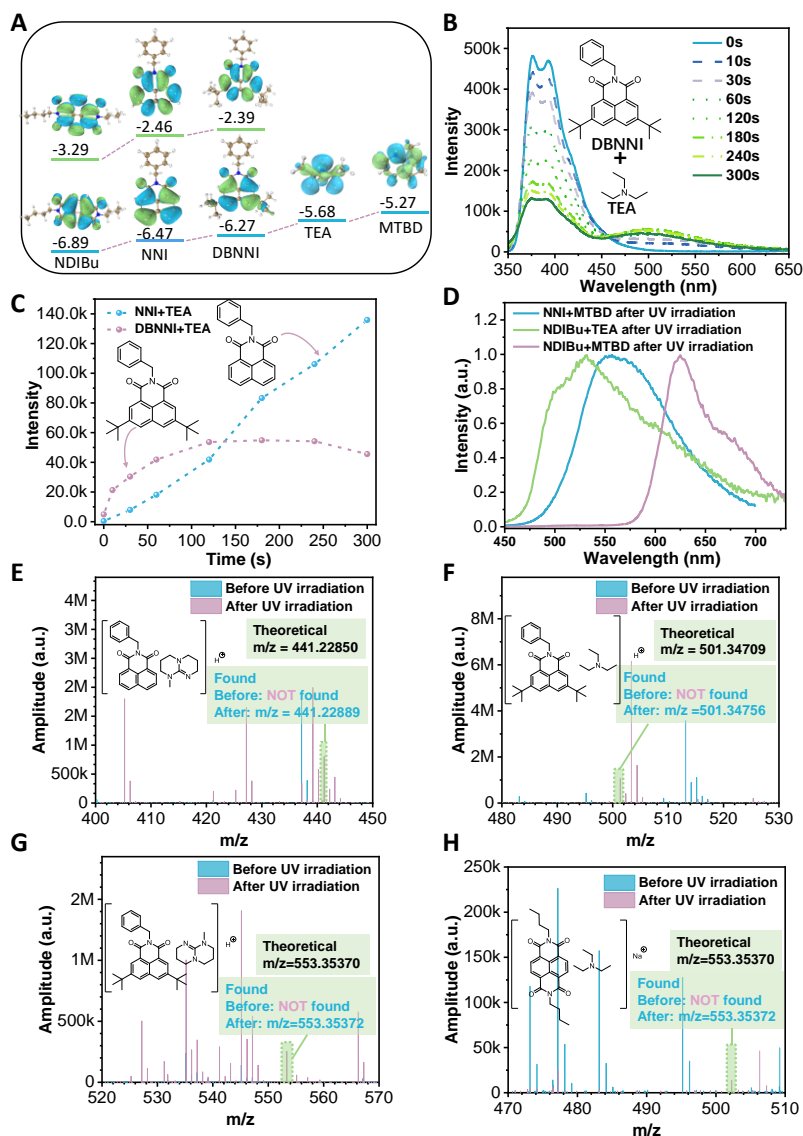


Figure 3. Properties modulation of PCTC

(A) HOMO-LUMO energy level of NDIBu, NNI, DBNNI, TEA, MTBD calculated at the B3LYP-D3BJ/6-31G (D, P) level in CH_3CN .

(B) Steady-state fluorescence emission spectra ($\lambda_{\text{ex}} = 335 \text{ nm}$) of DBNNI-TEA after different UV irradiation times in CH_3CN .

(C) Relationship of emission spectra intensity vs. UV irradiation time (recorded at 500 nm for NNI-TEA and DBNNI-TEA, NNI: $1 \times 10^{-4} \text{ M}$, DBNNI: $1 \times 10^{-4} \text{ M}$, TEA: 10 eq. in CH_3CN).

(D) Relationship steady-state fluorescence emission spectra of the NNI/MTBD mixture ($\lambda_{\text{ex}} = 335 \text{ nm}$), the NDIBu/TEA mixture ($\lambda_{\text{ex}} = 430 \text{ nm}$) and the NDIBu/MTBD mixture ($\lambda_{\text{ex}} = 430 \text{ nm}$) after UV irradiation.

(E-H) The HRMS graphs with designated m/z ranges for acetonitrile solutions of the NNI/MTBD mixture (E), the DBNNI/TEA mixture (F), the DBNNI/MTBD mixture (G), and the NDIBu/TEA mixture (H) before and after UV irradiation in CH_3CN . The solution samples were exposed to air immediately prior to and during the course of HRMS measurements (NNI: $1 \times 10^{-4} \text{ M}$, DBNNI: $1 \times 10^{-4} \text{ M}$, NDIBu: $1 \times 10^{-4} \text{ M}$, TEA: 10 eq., MTBD: 10 eq. in CH_3CN).

Properties modulation and theoretical studies on PCTCs

To back the conclusions from calculations, we synthesized two additional aromatic imides, NDIBu and DBNNI (Figure 3a). The first molecule is a diimide with a calculated HOMO energy level of -6.89 eV, a substantial decrease from that of NNI at -6.47 eV. The second imide has two tert-butyl groups on the 3 and 6 positions of the NNI ring, respectively, and has a LUMO level of -6.27 eV, a value still below that of the TEA at -5.68 eV. Since the calculations indicate that blocking the 4/5 positions would destroy the PCTC, as has been observed for NNINN, then blocking only the 3/6 positions should still allow for the PCTC generation as long as the LUMO of the imide is still lower than the amine. Indeed, it was observed that despite the steric hinderance from the two tert-butyl groups, a new photoluminescence band near 500 nm indicative of a PCTC between DBNNI and TEA could be recorded after UV radiation, consistent with the computational results of a complex near the 4/5 position (Figure 3b). However, the photoluminescence change as a function of irradiation time suggests that although the PCTC formation kinetics is not as deterred, its thermodynamic stability is compromised as equilibrium is more rapidly achieved for the [DBNNI-TEA] PCTC (Figure 3c and Figure S19). By introducing another amine of a completely different chemical structure and HOMO energy level (i.e., MTBD), the luminescent properties of the imide-amine PCTCs are can be systematically regulated. As shown in Figure 3d and Figure S20, a more powerful donor/acceptor combination could lead to redshift of the PCTC luminescence: NNI/MTBD (yellow, $\lambda_{PL} \sim 550$ nm, $\tau = 16.4$ ns), NDIBu/TEA (yellow-green, $\lambda_{PL} \sim 530$ nm, $\tau = 10.6$ ns) and NDIBu/MTBD (red, $\lambda_{PL} \sim 625$ nm, $\tau = 14.3$ ns) (Figure S21-22). These alleged PCTCs are also confirmed with HRMS except for UV treated NDIBu/MTBD (Figure S23 and Figure S39-43), which exhibits extraordinary sensitivity toward air during the sample injection. The color of the alleged [NDIBu-MTBD] PCTC rapidly dissipated immediately when the solution was withdrawn; we suspect that mechanical disturbance of the solution could also contribute to its dissociation in addition to oxygen. We also performed EPR spectroscopic measurements for the UV treated imide/amine solutions (Figure S24-27), and found that the [NNI-TEA] PCTC is the only complex that does not appear to undergo spontaneous dissociation at room temperature as the rest samples exhibit detectable EPR signals characteristic of the imide anion radical species. The $^1\text{H-NMR}$ spectra could corroborate the EPR results (Figure S28-30), where the NMR peaks were diminished when EPR signals were detected. Again, the results are consistent with the Marcus model, where the kinetic barrier is lowered when a more powerful donor/acceptor is used (Figure S31).³⁷ However, the absence of NMR spectral changes for the NNI-TEA PCTC does not necessarily exclude the possibility of a photo-induced, non-typical Meisenheimer complex, which is unstable at room temperature and could be in equilibrium with the radical pair. The possibility aligns with the significance of steric effects seen with substitutions at NNI's 5 position or with larger amines, potentially hastening the interconversion between radicals and the photo-induced Meisenheimer complex. A swift conversion between these two may not reflect in the NMR signals, yet the UV-Vis spectroscopy could still reveal the Meisenheimer-complex-like electronic structures, as photon absorption is a very fast process.

Based on the visual observation, spectroscopic data, and calculations, we provide a physical model for PCTC (Scheme 1b). First, the NNI and TEA become an attractive pair in the excited state upon UV excitation of the NNI, where the excited molecule NNI* diffuses to encounter a ground-state amine and forms an excited-state CT pair [NNI-TEA]*. Then, the metastable [NNI-TEA]* decays to the ground state to yield the proposed PCTC structure [NNI-TEA] via the emission of a much red-shifted photon (by ~ 0.57 eV) compared to that of NNI*. The photoluminescence is essentially an exciplex in nature, except that for an exciplex, the ground-state pair becomes repulsive or weakly attractive, and rapidly dissociates in solution at room temperature. Finally, the ground-state [NNI-TEA] appears to be in a kinetically trapped state, since the PCTC cannot by itself dissociates into free-moving NNI and TEA in solution. It is, however, not clear how molecular oxygen is required to catalyze the dissociation of PCTC with the possibility of reacting with one of the two components to give rise to trace oxidation products.

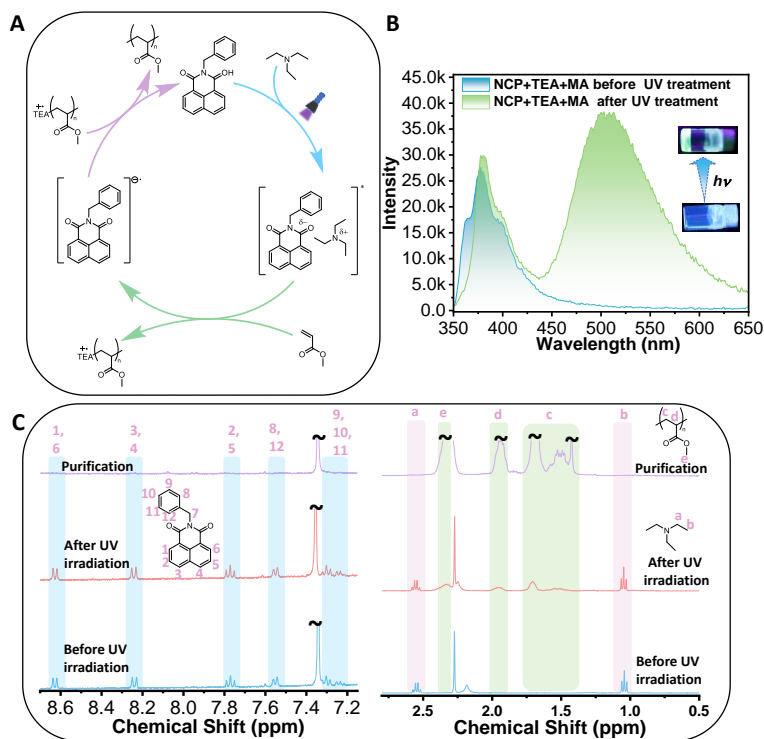


Figure 4. Initiation and Catalytic Photopolymerization of Acrylate

(A) The proposed photocatalytic cycle of PCTC-activated methacrylate (MA) polymerization.

(B) Steady-state fluorescence emission spectra ($\lambda_{\text{ex}} = 335 \text{ nm}$) of MA (2 mL) in the presence of NNI (0.25%) and TEA (1%) before and after UV irradiation under Ar at room temperature.

(C) $^1\text{H-NMR}$ spectra of MA in the presence of NNI (0.25%) before and after UV radiation for 60 s and purified PMA in CDCl_3 ($\lambda = 365 \text{ nm}$).

Initiating and catalyzing acrylate photopolymerization

Since CTCs are *a priori* “high-energy complexes” under inert atmospheres and are experimentally prone to heterogeneous dissociation to produce a pair of radicals (e.g., $\text{TEA}^{+\bullet}$ and $\text{NNI}^{\bullet-}$) when subjected to the presence of other reactants, they could potentially be used to initiate methyl acrylate (MA) polymerization, as an exploratory application (Figure 4a). As shown in Figure 4b, NNI and TEA were added to neat MA at a mass ratio 0.25 : 1 : 100 (NNI: TEA: MA). Prior to UV treatment, the mixture showed no observable interactions and no detectable polymerization; when the mixed liquids were exposed to 365 nm LED light (at a power density of $\sim 150 \text{ mW/cm}^2$), strong green fluorescence characteristic of PCTC immediately appeared ($\lambda_{\text{em}} = 500 \text{ nm}$, $\tau_{\text{F}} = 15.0 \text{ ns}$, Figure S32). The viscosity of the mixture simultaneously increased sharply, and the conversion was calculated by $^1\text{H-NMR}$ to be $>30\%$ within 1 min. On the contrary, no visible change in viscosity could be noted for the MA liquid with the presence of only either the imide (NNI: MA = 0.25: 100) or the amine (TEA: MA = 1: 100), where the $^1\text{H-NMR}$ signals show that there was essentially no polymerization of the MA monomer under the same condition. Figure 4c shows a magnified $^1\text{H-NMR}$ signal of the NNI/TEA/MA (0.25:1:100) mixture prior to and after photo-polymerization: no chemical changes could be detected for NNI but the characteristic signals of MA are converted to those of the PMA polymer (Figure S33-37). The MALDITOF spectrometry data show that the molecular weight of the end groups of PMA matches that of TEA (Figure S38), suggesting that $\text{TEA}^{+\bullet}$, which is heterogeneously cleaved from the PCTC, is most likely the initiator for MA.

Carbon dioxide catalytic reduction

The photo-polymerization mainly takes advantage of the amine radical cation (e.g., $\text{TEA}^{+\bullet}$) which oxidizes the acrylate to yield the propagating species. On the other hand, the dissociated radical anion (e.g., $\text{NNI}^{\bullet-}$) can be used for reduction reactions due to its

strong reducing ability.³⁸ As shown in Figure 6a, the CO₂ gas was used to purge the NNI/MTBD solution (CH₃CN) for 30 min to reach an equilibrium condition. The calculated CO₂ concentration after purging, was 0.282 mol/L in CH₃CN. The treated solution was then sealed by a rubber septum with a stir bar under UV irradiation ($\lambda_{\text{ex}} = 365$ nm, 10-W LED light) at room temperature. The conversion of CO₂ into HCOOH was present from the NMR spectroscopy: new signals from NMR (¹H-NMR and ¹³C-NMR) appeared after the CO₂-purged NNI/MTBD mixture solution was irradiated with UV light. By comparing the post-reaction NMR spectra with that of standard formic acid, the newly generated substance was most likely formic acid as well given the perfect spectral match (Figure 6b, Figure 6c and Figure S44-45). Throughout the entirety of the photoconversion process, NNI can serve as a photocatalyst with MTBD acting as sacrificial electron donors.³⁹ However, the initial formation of the PCTC can significantly increase the energy level of the NNI species, which is elevated to an upper excited state upon absorption of a second photon. The protons in the formic acid product are believed to be contributed from the solvent (e.g., a trace amount of water or abstraction from CH₃CN). Consequently, the PCTC allows carbon dioxide conversion (23.2 $\mu\text{mol}\cdot\text{g}^{-1}\cdot\text{h}^{-1}$, mesitylene was used as the internal reference for HCOOH yield calculation, Figure S46) to be achieved by irradiation with a very low power light source (10 W) under ambient conditions (room temperature, 1 atm, in general reaction vessels), without the use of a metal-containing catalyst.

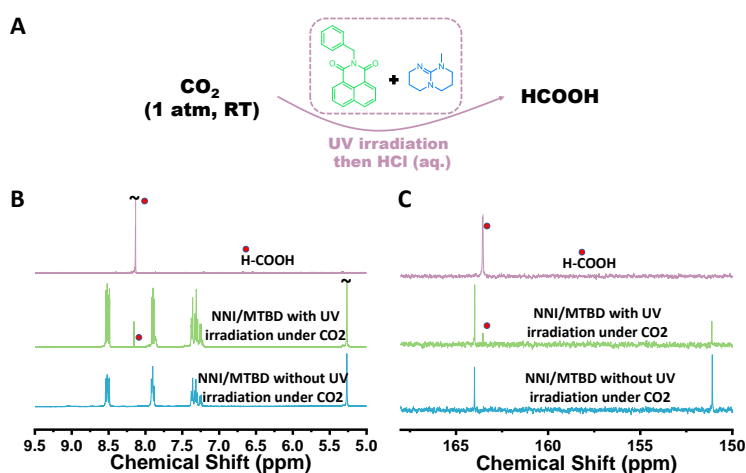


Figure 5. Photoconversion of carbon dioxide

(A) Schematic diagram of photoconversion of carbon dioxide to formic acid (HCOOH) using the amine-imide PCTC.

(B) ¹H-NMR spectra (DMSO-*d*₆) of the NNI/MTBD mixture with and without UV irradiation under CO₂, and ¹H-NMR spectra (DMSO-*d*₆) of formic acid (HCOOH).

(C) ¹³C-NMR spectra (DMSO-*d*₆) of the NNI/MTBD mixture with and without UV irradiation under CO₂, and ¹³C-NMR spectra (DMSO-*d*₆) of formic acid (HCOOH).

UV light energy storage and release

Since the NNI-MTBD PCTC is solution-stable provided that it is sealed under inert atmosphere such as argon, it may be used as a high-energy chemical to “on-demand” photochemical products without the use of UV light. In this sense, the PCTC serves as a medium for harvesting and releasing stored UV light energy at room temperature. To test this hypothesis, we devised an experiment to show how a photochromic product from colorless to pink could be obtained without direct UV radiation (Figure 6a and Figure S47). The high-energy PCTC was first prepared after an acetonitrile solution of NNI and MTBD was treated with UV light; the PCTC solution was stored at room temperature under argon for 7 d prior to use (Figure S48-50). The photochromic reaction was first reported by Izawa et al.⁴⁰ using a nitrate-substituted NNI (NO₂NNI), which turns into pink-colored anions upon UV exposure in the presence of an electron donor molecule such as the succinate anion. The pink color is obviously necessitated by light; here we demonstrate that it is not. After the addition of the PCTC stock solution to the NO₂NNI solution in the dark, a noticeable color change from colorless to pink occurred; an identical color change process was also observed when the NO₂NNI/MTBD mixed solution was exposed to UV light. Spectroscopic data (¹H-NMR and EPR) were collected to quantitatively compare the two pathways toward photochromism (Figure S51). As

illustrated in Figure 6B, the ^1H NMR signals of the NNI (on the naphthalene ring) disappeared in the post-UV NNI/MTBD PCTC solution, indicating the formation of NNI anionic radicals (NNI^-). Interestingly, when NO_2NNI was added to the PCTC solution in the dark, reappearance of the ^1H NMR signals for NNI, accompanied by the concomitant disappearance of ^1H NMR signals of NO_2NNI aromatic protons (Figure S52) was recorded, suggesting the dissociation of PCTC and generation of NO_2NNI anionic radicals (NO_2NNI^-). As a control experiment, when NO_2NNI was added to the non-irradiated NNI/MTBD mixed solution, ^1H NMR signals (NNI and NO_2NNI) remained unchanged, suggesting the chromic reaction is not accessible at room temperature without light. The EPR data further corroborated this process (Figure S53), i.e., when NO_2NNI was added to the PCTC solution (NNI/MTBD) in the dark, the NNI radical signal started to transition into that of NO_2NNI /MTBD after UV radiation.

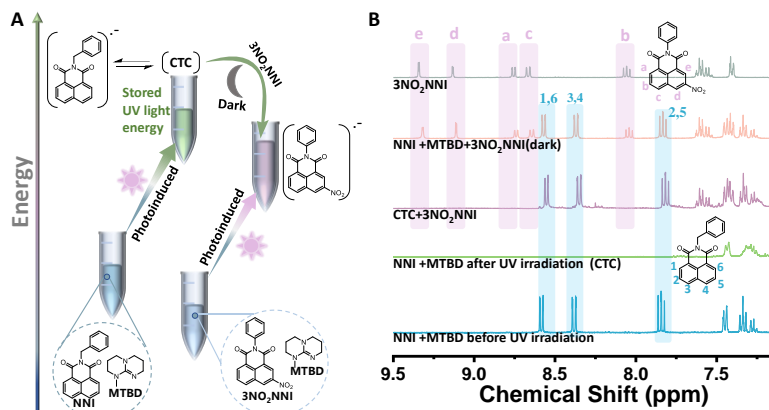


Figure 6. UV energy storage and release

(A) Schematic illustration of an alternative dark (moon symbol) pathway toward a photochromic product, which is conventionally achieved via a light (sun symbol) radiation pathway. The dark pathway first employs the light-generated, highly reactive NNI-MTBD PCTC in organic solution, which is transferred to the NO_2NNI to instantly yield the photochromic product at a later time.

(B) ^1H NMR spectra (CD_3CN) demonstrating the aromatic signal changes associated the dissociation of PCTC and generation of NO_2NNI radical anions.

CONCLUSIONS

In summary we have presented the chain of evidence to support the existence of a previously unreported chemical species formed between a naphthalimide derivative and a tertiary amine after UV irradiation, i.e., a “photo-induced charge-transfer complex (PCTC)”. Such a PCTC is believed to first go through an exciplex state, and then relax into a solution stable complex that is otherwise inaccessible from the ground state. The most direct evidence from HRMS reveals that the PCTC is created in a 1:1 ratio between the NNI and the amine molecules. The other spectroscopic techniques, however, suggest that the PCTC is either not or weakly connected through a chemical bond, and is rather similar to a weaker version of the Meisenheimer complex, backed by theoretical calculations. We have recently shown that complexation between two organic molecules do not necessarily induce significant changes in their NMR spectra but can change the electronic structure of the pair entirely manifested by calorimetry, UV-Vis absorption and luminescence methods. Taking advantage of the high ground-state energy level and chemical reactivity of the PCTC, we were able to use it to initiate the catalytic polymerization of methyl methacrylate, realize the photoconversion of carbon dioxide under ambient conditions, and demonstrate the possibility of an alternative dark pathway for photochromic products using a PCTC as a conduit for photon energy storage and on-demand release. Through these experiments, we showcase the potential of PCTC as a versatile and purely organic agent in various chemical processes. We anticipate that PCTCs are likely to expand the scope of photochemistry in organic syntheses using building blocks from many different core chemical structures.

EXPERIMENTAL PROCEDURES

Resource availability

Lead contact

Further information and requests for resources should be directed to and will be fulfilled by the lead contact, Guoqing Zhang (gzhang@ustc.edu.cn).

Materials availability

This study did not generate new materials.

Data and code availability

All data needed to support the conclusions of this manuscript are included in the main text and/or the supplemental information.

ACKNOWLEDGMENTS

We thank the Fundamental Research Funds for the Central Universities (WK9990000099 to G. Z.), Innovation Program for Quantum Science and Technology (2021ZD0303301) and for financial support. This research was also supported by the advanced computing resources provided by the Supercomputing Center of the USTC.

AUTHOR CONTRIBUTIONS

G.Z. and W.H. designed the experiments and wrote the paper. W.H. and X.Z. carried out the synthesis. W.H. performed spectroscopic measurements. G.Z., W.H., J.J. and B.C. discussed the results and edited the manuscript. G.Z., W.H., B.C. and B.Z. analyzed the data. W.H. and A.F. performed high-resolution mass spectrometry measurements. G.Z., W.H. and H.S. conducted computational work and theoretical analysis. The project was supervised by G.Z.

DECLARATION OF INTERESTS

The authors declare no competing interests.

REFERENCES

1. Srimuk, P., Su, X., Yoon, J., Aurbach, D., and Presser, V. (2020). Charge-transfer materials for electrochemical water desalination, ion separation and the recovery of elements. *Nat. Rev. Mater.* 5, 517-538. <https://doi.org/10.1038/s41578-020-0193-1>.
2. Foster, R. (1980). Electron donor-acceptor complexes. *J. Phys. Chem.* 84, 2135-2141. <https://doi.org/10.1021/j100454a006>.
3. Wang, Z., Hao, A., and Xing, P. (2023). Charge-Transfer Complex Doped Photothermal Hydrogels for Discriminating Circularly Polarized Near-Infrared Light. *Angew. Chem. Int. Ed.* 62, e202214504. <https://doi.org/10.1002/anie.202214504>.
4. Wang, W., Luo, L., Sheng, P., Zhang, J., and Zhang, Q. (2021). Multifunctional features of organic charge-transfer complexes: advances and perspectives. *Chem. Eur. J.* 27, 464-490. <https://doi.org/10.1002/chem.202002640>.
5. Sarma, M., and Wong, K.-T. (2018). Exciplex: an intermolecular charge-transfer approach for TADF. *ACS Appl. Mater. Interfaces* 10, 19279-19304. <https://doi.org/10.1021/acsami.7b18318>.
6. Nishimura, N., Lin, Z., Jinnai, K., Kabe, R., and Adachi, C. (2020). Many exciplex systems exhibit organic long-persistent luminescence. *Adv. Funct. Mater.* 30, 2000795. <https://doi.org/10.1002/adfm.202000795>.
7. Lima, C.G., de M. Lima, T., Duarte, M., Jurberg, I.D., and Paixao, M.W. (2016). Organic synthesis enabled by light-irradiation of EDA complexes: theoretical background and synthetic applications. *ACS Catal.* 6, 1389-1407. <https://doi.org/10.1021/acscatal.5b02386>.
8. Crisenza, G.E., Mazzarella, D., and Melchiorre, P. (2020). Synthetic methods driven by the photoactivity of electron donor-acceptor complexes. *J. Am. Chem. Soc.* 142, 5461-5476. <https://doi.org/10.1021/jacs.0c01416>.
9. Fu, M.-C., Shang, R., Zhao, B., Wang, B., and Fu, Y. (2019). Photocatalytic decarboxylative alkylations mediated by triphenylphosphine and sodium iodide. *Science* 363, 1429-1434. <https://doi.org/10.1126/science.aav3200>.
10. Kohara, K., Trowbridge, A., Smith, M.A., and Gaunt, M.J. (2021). Thiol-mediated α -amino radical formation via visible-light-activated ion-pair charge-transfer complexes. *J. Am. Chem. Soc.* 143, 19268-19274.

<https://doi.org/10.1021/jacs.1c09445>.

11. Uchikura, T., Oshima, M., Kawasaki, M., Takahashi, K., and Iwasawa, N. (2020). Supramolecular Photocatalysis by Utilizing the Host–Guest Charge-Transfer Interaction: Visible-Light-Induced Generation of Triplet Anthracenes for [4+ 2] Cycloaddition Reactions. *Angew. Chem. Int. Ed.* 59, 7403-7408. <https://doi.org/10.1002/anie.201916732>.
12. Wang, H., Wu, J., Noble, A., and Aggarwal, V.K. (2022). Selective Coupling of 1, 2-Bis-Boronic Esters at the more Substituted Site through Visible-Light Activation of Electron Donor–Acceptor Complexes. *Angew. Chem. Int. Ed.* 134, e202202061. <https://doi.org/10.1002/anie.202202061>.
13. Siu, J.C., Parry, J.B., and Lin, S. (2019). Aminoxyl-catalyzed electrochemical diazidation of alkenes mediated by a metastable charge-transfer complex. *J. Am. Chem. Soc.* 141, 2825-2831. <https://doi.org/10.1021/jacs.8b13192>.
14. Kodo, T., Nagao, K., and Ohmiya, H. (2022). Organophotoredox-catalyzed semipinacol rearrangement via radical-polar crossover. *Nat. Commun.* 13, 2684. <https://doi.org/10.1038/s41467-022-30395-4>.
15. Schleper, A.L., Goushi, K., Bannwarth, C., Haehnle, B., Welscher, P.J., Adachi, C., and Kuehne, A.J. (2021). Hot exciplexes in U-shaped TADF molecules with emission from locally excited states. *Nat. Commun.* 12, 6179. <https://doi.org/10.1038/s41467-021-26439-w>.
16. Tan, S., Jinnai, K., Kabe, R., and Adachi, C. (2021). Long-persistent luminescence from an exciplex-based organic light-emitting diode. *Adv. Mater.* 33, 2008844. <https://doi.org/10.1002/adma.202008844>.
17. Schwarze, M., Gaul, C., Scholz, R., Bussolotti, F., Hofacker, A., Schellhammer, K.S., Nell, B., Naab, B.D., Bao, Z., and Spoltore, D. (2019). Molecular parameters responsible for thermally activated transport in doped organic semiconductors. *Nat. Mater.* 18, 242-248. <https://doi.org/10.1038/s41563-018-0277-0>.
18. Tang, X., Cui, L.-S., Li, H.-C., Gillett, A.J., Auras, F., Qu, Y.-K., Zhong, C., Jones, S.T., Jiang, Z.-Q., and Friend, R.H. (2020). Highly efficient luminescence from space-confined charge-transfer emitters. *Nat. Mater.* 19, 1332-1338. <https://doi.org/10.1038/s41563-020-0710-z>.
19. Coropceanu, V., Chen, X.-K., Wang, T., Zheng, Z., and Brédas, J.-L. (2019). Charge-transfer electronic states in organic solar cells. *Nat. Rev. Mater.* 4, 689-707. <https://doi.org/10.1038/s41578-019-0137-9>.
20. Schreiber, C.L., and Smith, B.D. (2019). Molecular conjugation using non-covalent click chemistry. *Nat. Rev. Mater.* 3, 393-400. <https://doi.org/10.1038/s41570-019-0095-1>.
21. Marcus, R.A. (1993). Electron transfer reactions in chemistry. Theory and experiment. *Rev. Mod. Phys.* 65, 599. <https://doi.org/10.1103/RevModPhys.65.599>.
22. Gopikrishna, P., Meher, N., and Iyer, P.K. (2017). Functional 1, 8-naphthalimide AIE/AIEEgens: recent advances and prospects. *Appl. Mater. Interfaces* 10, 12081-12111. <https://doi.org/10.1021/acsami.7b14473>.
23. Li, Y., Zhao, Z., Zhang, J., Kwok, R.T., Xie, S., Tang, R., Jia, Y., Yang, J., Wang, L., and Lam, J.W., et al. (2018). A bifunctional aggregation-induced emission luminogen for monitoring and killing of multidrug-resistant bacteria. *Adv. Funct. Mater.* 28, 1804632. <https://doi.org/10.1002/adfm.201804632>.
24. Sun, S., Wang, J., Ma, L., Ma, X., and Tian, H. (2021). A universal strategy for organic fluid phosphorescence materials. *Angew. Chem. Int. Ed.* 60, 18557-18560. <https://doi.org/10.1002/anie.202107323>.
25. Chen, B., Huang, W., and Zhang, G. (2023). Observation of Chiral-selective room-temperature phosphorescence enhancement via chirality-dependent energy transfer. *Nat. Commun.* 14, 1514. <https://doi.org/10.1038/s41467-023-37157-w>.
26. Roos, L., Malan, F.P., and Landman, M. (2021). Naphthalimide-NHC complexes: Synthesis and properties in catalytic, biological and photophysical applications. *Coord. Chem. Rev.* 449, 214201. <https://doi.org/10.1016/j.ccr.2021.214201>.
27. Huang, W., Zhang, X., Chen, J., Zhang, B., Chen, B., and Zhang, G. (2023). Organic Photocatalyzed Polyacrylamide without Heterogeneous End Groups: A Mechanistic Study. *ACS Catal.* 13, 2542-2546. <https://doi.org/10.1021/acscatal.2c05972>.
28. Zhang, Y.-Y., and Zhou, C.-H. (2011). Synthesis and activities of naphthalimide azoles as a new type of antibacterial and antifungal agents. *Bioorganic Med. Chem. Lett.* 21, 4349-4352. <https://doi.org/10.1016/j.bmcl.2011.05.042>.
29. Chen, X., Xu, C., Wang, T., Zhou, C., Du, J., Wang, Z., Xu, H., Xie, T., Bi, G., and Jiang, J. (2016). Versatile room-temperature-phosphorescent materials prepared from N-substituted naphthalimides: emission enhancement and chemical conjugation. *Angew. Chem. Int. Ed.* 55, 9872-9876. <https://doi.org/10.1002/anie.201601252>.
30. Huang, W., Chen, B., and Zhang, G. (2019). Persistent Room-Temperature Radicals from Anionic Naphthalimides: Spin Pairing and Supramolecular Chemistry. *Chem. Eur. J.* 25, 12497-12501. <https://doi.org/10.1002/chem.201902882>.
31. Pellegrin, Y., and Odobel, F. (2017). Sacrificial electron donor reagents for solar fuel production.

- C. R. Chimie 20, 283-295.
<https://doi.org/10.1016/j.crci.2015.11.026>
32. Rieth, A.J., Gonzalez, M.I., Kudisch, B., Nava, M., and Nocera, D.G. (2021). How radical are “radical” photocatalysts? A closed-shell Meisenheimer complex is identified as a super-reducing photoreagent. *J. Am. Chem. Soc.* 143, 14352-14359.
<https://doi.org/10.1021/jacs.1c06844>
33. Zhang, X., Du, J., Liao, F., Su, H., Zhang, X., Miao, H., and Zhang, G. (2021). Phosphorescence Enables Identification of Electronic State for Acridinium Salt in Solutions. *J. Phys. Chem. Lett.* 12, 12242-12248.
<https://doi.org/10.1021/acs.jpclt.1c03584>
34. Zhang, J., and Lu, T. (2021). Efficient evaluation of electrostatic potential with computerized optimized code. *Phys. Chem. Chem. Phys.* 23, 20323-20328.
<https://doi.org/10.1039/D1CP02805G>
35. Lu, T., and Chen, F. (2012). Multiwfn: A multifunctional wavefunction analyzer. *J. Comput. Chem.* 33, 580-592.
<https://doi.org/10.1002/jcc.22885>
36. Johnson, E.R., Keinan, S., Mori-Sánchez, P., Contreras-García, J., Cohen, A.J., and Yang, W. (2010). Revealing noncovalent interactions. *J. Am. Chem. Soc.* 132, 6498-6506.
<https://doi.org/10.1021/ja100936w>
37. Silverstein, T.P. (2012). Marcus theory: thermodynamics CAN control the kinetics of electron transfer reactions. *J. Chem. Educ.* 1159-1167.
<https://doi.org/10.1021/ed1007712>
38. Tian, X., Karl, T.A., Reiter, S., Yakubov, S., de Vivie-Riedle, R., König, B., and Barham, J.P. (2021). Electro-mediated PhotoRedox Catalysis for Selective C(sp³)-O Cleavages of Phosphinated Alcohols to Carbanions. *Angew. Chem. Int. Ed.* 60, 20817-20825.
<https://doi.org/10.1002/anie.202105895>
39. Oh, Y., and Hu, X. (2013). Organic molecules as mediators and catalysts for photocatalytic and electrocatalytic CO₂ reduction. *Chem. Soc. Rev.* 42, 2253-2261.
<https://doi.org/10.1039/C2CS35276A>
40. Izawa, H., Yasufuku, F., Nokami, T., Ifuku, S., Saimoto, H., Matsui, T., Morihashi, K., and Sumita, M. (2021). Unique photophysical properties of 1, 8-naphthalimide derivatives: Generation of semi-stable radical anion species by photo-induced electron transfer from a carboxy Group. *ACS omega* 6, 13456-13465.
<https://doi.org/10.1021/acsomega.1c01685>